Ecological Processes

RESEARCH

Open Access

Influence of soil properties on selenium concentration in paddy soil and rice grains in the hilly regions of southern China

Guiduo Shang[1], Weijun Zhou[1*], Rui Liu[1], Yuzhou Zhou[1], Zhangqian Xu[1], Haojie Cui[1] and Yixiang Cai[2]

Abstract

Background Selenium (Se) is essential for human health and is predominantly obtained from dietary sources, particularly rice in Hunan Province, a significant rice-producing region in southern China. Investigating the relationship between Se levels in paddy soil and rice grains, along with the associated influencing factors, is critical for enhancing Se-enriched food security.

Results Analysis of 128,992 samples collected between 2019 and 2022 revealed that the soil Se concentration in Hunan exceeded the global average, with rice grains showing promising potential for Se enrichment. Various analytical methods, including statistical analyses, co-occurrence networks, and correlation heatmaps, were utilized to scrutinize the extensive dataset. Additionally, partial least squares path analysis elucidated the interactive effects of influencing factors on soil Se concentration, rice grain Se concentration, and Se bioconcentration factor (BCF). Soil parent materials significantly affected soil Se concentration, rice grain Se concentration, and Se BCF ($p < 0.01$). Factors such as soil cation exchange capacity, soil organic matter, slope, and soil concentrations of Cu, Mn, and Zn demonstrated positive correlations with soil Se concentration. Similarly, these factors exhibited positive associations with rice grain Se concentration. Conversely, negative correlations were observed between certain factors and Se BCF. As a result, predictive models were developed for soil Se, rice grain Se concentration, and Se BCF.

Conclusions This study contributes valuable insights to inform policy-making for Se-enriched food production and to ensure regional nutritional equilibrium. Caution is recommended in areas with excessive Se levels to prevent potential poisoning risks.

Keywords Bioconcentration factor, Biofortification, Parent material, Organic matter, Se in soil and rice, Big data

*Correspondence:
Weijun Zhou
wjzh0108@163.com
[1] College of Resources, Hunan Agricultural University, Changsha 410028, People's Republic of China
[2] Key Laboratory of Agro-Ecological Processes in Subtropical Regions, Changsha Research Station for Agricultural and Environmental Monitoring, Institute of Subtropical Agriculture, Chinese Academy of Sciences, Changsha 410125, People's Republic of China

Introduction

Selenium (Se) plays a crucial role in certain physiological processes in the human body and is an important trace element for maintaining human health (Yang et al. 2022). Adequate Se intake can enhance the immune system, anti-aging abilities, reduce heavy metal toxicity, and protect cardiovascular and hepatic functions, among others. Conversely, both inadequate and excessive Se intake can lead to a range of diseases (Kieliszek et al. 2022; Natasha et al. 2018; Yang et al. 1983). Therefore, understanding the Se concentration in food, balancing dietary choices, and controlling Se intake have positive implications for maintaining health (Qvarforth et al. 2022; Hawrylak-Nowak et al. 2015).

Se is primarily obtained by humans through plants (e.g., wheat, rice, maize) in the food chain. Rice, which is a staple food in southern China, serves as a significant Se source (Ning et al. 2022; Song et al. 2022). Therefore, understanding the Se concentration and influencing factors in rice grains is crucial for the development and utilization of soil Se resources in agricultural fields. As a fundamental element reservoir, soil is pivotal in the geochemical cycling of surface ecosystem elements, providing vital nutrients for plant growth (Rayman 2002). Accordingly, soil serves as the principal source of Se in plants (Favorito et al. 2017). However, Se distribution in soil exhibits substantial disparities, displaying pronounced spatial variability (Beladel et al. 2013). Global soil Se concentration averages 0.4 mg·kg^{-1} (Fordyce 2007), with 0.29 mg·kg^{-1} in China, indicating a significant deviation from the global norm (Tan et al. 2002). Approximately 51% of China's regions exhibit varying degrees of Se deficiency (Dinh et al. 2018). In light of this, exploring aspects such as soil Se concentration, Se concentration in rice grains, the relationship between soil and rice grain Se, spatial distribution patterns, and the underlying influencing factors holds great potential for the scientific and efficient utilization of natural Se-rich resources. This endeavor bears immense significance in enhancing Se intake for the Chinese population and promoting national health.

In recent years, a plethora of studies has extensively explored the spatial distribution of Se in both soil and rice grains, investigating various influencing factors and yielding noteworthy discoveries. Prior research suggests that the parent material plays a pivotal role in regulating soil Se (Fordyce et al. 2007). For example, black shales, rich in Se, act as substrates for numerous Se-rich soils in America (Elrashidi 2018), with similar occurrences in Wales and Ireland (Davies and Houghton 1983). Further investigations reveal that diverse soil physicochemical properties, such as pH (Yang et al. 2022; Xu et al. 2018), soil organic matter, essential micronutrients, topography (Xu et al. 2018), and climatic conditions, impact soil Se, plant Se, and Se bioavailability. Notably, Li et al. (2017) and Dinh et al. (2017) propose a dual influence of organic matter on soil Se efficacy, with a more significant presence of organic matter enhancing soil Se availability in lower pH soil conditions and diminishing it in higher pH soil environments. These studies encompass a wide range of environmental contexts, including urban areas, hills, mountainous regions, plains, and river basins (Liu et al. 2018), and vary in spatial scales, ranging from nationwide to provincial, municipal, and county-level analyses (Hao et al. 2021). Many of these studies primarily focus on the isolated impact of individual factors or a subset of factors (Kushwaha et al. 2022). There is limited comprehensive analysis of the combined influence of soil parent material, soil properties, geographical factors, climate parameters, and plant micronutrients on the distribution and accumulation of Se in paddy soils and rice grains. It is essential to conduct in-depth analyses and explore the impact of multiple factors. A regional perspective, abundant data resources, and high-precision methods should be employed to study the distribution of Se in soil-rice systems at a regional level.

Hunan Province, renowned as a prominent rice cultivation region in China (Zou et al. 2021; Wang et al. 2019), was selected as the primary focus of this study. In this study, a dataset encompassing a large number of samples of paddy soils, rice grains, and environmental parameters from Hunan Province was examined. The analysis considered soil parent material, chemical properties [soil organic matter (SOM), cation exchange capacity (CEC), and pH], geographical and climatic variables [elevation, slope, aspect, distance from water areas (DFW), mean annual temperature (MAT), and mean annual precipitation (MAP)], as well as critical trace elements (Zn, Cu, and Mn) present in both paddy soil and rice grains. The aim was to determine the spatial distribution and accumulation patterns of Se in paddy soils and rice grains in Hunan Province, elucidating the multifaceted impacts of various environmental variables on Se accumulation in both paddy soils and rice grains.

Materials and methods

Study area

This study was carried out in Hunan Province, which is located in southern China and encompasses the southern segment of the middle reaches of the Changjiang River (Yangtze River). Geographically, it extends longitudinally from approximately 108°47′E to 114°15′E and latitudinally from around 24°38′N to 30°08′N (Fig. 1). The province encompasses a total land area of 211,800 km^2, with a cultivated land area spanning 37,081 km^2. Among these, paddy fields occupy 30,710 km^2, while dry land covers an area of 6371 km^2. Characterized by a monsoonal subtropical climate, the region witnesses an annual temperature range averaging from 16.0 to 18.5 °C and annual precipitation ranging from 1200 to 1700 mm (Pan et al. 2022). The province exercises jurisdiction over 13 cities, one autonomous prefecture, and 122 counties or districts. Positioned in the transitional terrain from the Yungui Plateau to the hilly terrain of Jiangnan, and from the mountainous region of Nanling to the plains of Jianghan, the study locale predominantly features mountainous and hilly topography.

Sampling and analyses

Sample collection and pretreatment

Between 2019 and 2022, a comprehensive collection effort encompassed a total of 128,992 paired soil-rice sites across Hunan Province. This extensive sampling endeavor was executed by the local eco-environmental management authority (Fig. 1). However, it's important to note that due to the survey design, certain sampling sites were not subject to a complete assessment of both paddy soil and rice grain properties. Specifically, attributes like SOM, soil pH, and Se concentration were assessed for all sites in both paddy soil and rice grains. On the other hand, the evaluation of parameters including soil Cu, Zn, and Mn concentration, rice Cu, Zn, and Mn concentration, along with CEC, was selectively conducted. The resultant data were compiled and summarized in Table 1.

During the sampling process, we collected topsoil samples (0–20 cm depth) using the double diagonal method as part of a 5-point mixed sampling approach, with each sample weighing over 2500 g (Pan et al. 2022). Similarly, rice grain samples were gathered in quintuplicate utilizing stainless steel scissors, and these samples were then aggregated to establish representative rice grain samples. These samples were stored within numbered plastic bags to maintain their distinctiveness. Subsequently, within the laboratory setting, paddy soil samples were allowed to air dry under room temperature conditions, homogenized via the use of a mortar and pestle, and then subjected to a series of sieving steps with mesh sizes of 2 mm and 0.145 mm to determine the chemical properties of the soil. A three-step washing procedure was employed for rice grain samples, entailing initial rinsing to eliminate soil particles and extraneous matter, followed by air-drying and hull removal, and concluding with the grinding of husk-free rice grains. Global Positioning System (GPS) technology was harnessed for precise geolocation of the sampling points.

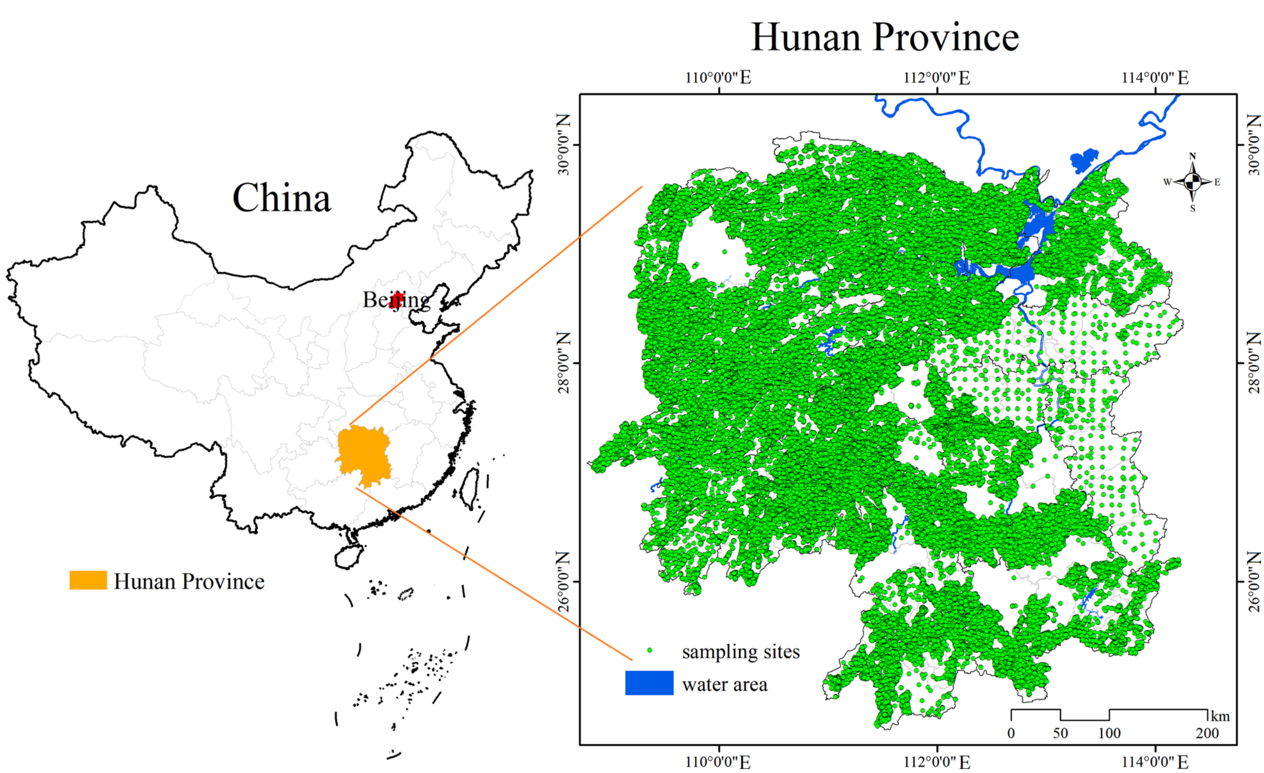

Fig. 1 Map of research area and sampling sites in Hunan Province, China

Table 1 Descriptive statistics of chemical properties of paddy soil and rice grains as well as climatic variables

Properties	*n*	Min	Median	Max	Mean	SD	CV (%)
Se_soil (mg·kg^{-1})	128,992	0.005	0.46	29.2	0.55	0.46	84.26
Se_grain (mg·kg^{-1})	128,992	0.001	0.046	3.312	0.058	0.12	199.52
Bioconcentraion factor (BCF)	128,992	0.00007	0.10	19.6	0.12	0.19	156.45
Soil pH	128,992	2.94	5.67	8.96	6.02	1.09	18.10
SOM (g·kg^{-1})	128,992	2.56	32.3	142	33.74	13.09	38.81
CEC (cmol·kg^{-1})	126,416	1.256	11.91	43.2	12.62	4.82	38.17
Zn_soil (mg·kg^{-1})	126,117	7.6	94.598	970.38	103.99	119.56	114.97
Mn_soil (mg·kg^{-1})	56,870	25.69	323.734	29,206	464.62	583.99	125.83
Cu_soil (mg·kg^{-1})	126,117	1.7	27.8	2230	30.69	38.24	124.58
Zn_grain (mg·kg^{-1})	126,117	0.25	14.3	426.14	13.87	6.05	43.59
Mn_grain (mg·kg^{-1})	54,628	0.05	9.24	105.47	9.12	5.77	63.24
Cu_grain (mg·kg^{-1})	126,117	0.025	2.054	51.61	2.15	1.72	79.88
MAP (mm)	128,992	1078	1279	2595	1690	310	18.31
MAT (°C)	128,992	10.5	17.6	20.2	17.5	1.37	7.81

Chemical analysis for paddy soil and rice grains

The paddy soil's pH and SOM were determined using titration and glass electrode methods, following the instructions provided in Ahmad et al. (2017). The CEC of the paddy soil samples was determined using the standard extraction solution method. To determine the concentration of Cu, Zn, and Mn in the paddy soil, we digested dried soil samples with a HNO_3 (65–68%) and $HClO_4$ (70–72%) mixture at a 4:1 volumetric ratio using a microwave digestion system. For rice grain samples, a comparable digestion procedure using a 4:1 volumetric ratio of HNO_3 (65–68%) to $HClO_4$ (70–72%) was employed, and the Se, Cu, Zn, and Mn concentrations were quantified using ICP-MS technique, according to the procedures described in Xu et al. (2020). To ensure the reliability and quality of our experiments, we used standard reference soil (GBW07410) and rice grain (GBW10010) samples from the China National Standard Material Resource Platform for soil and plant sample analysis.

Data sources

The elevation dataset (DEM) with a spatial resolution of 30 m was obtained from the China Geospatial Data Cloud (Liu et al. 2021b). Mean annual temperature and annual precipitation data (MAT and MAP) were obtained from the Chinese Academy of Sciences, accessible at http://www.resdc.cn (Xiao et al. 2020b). Information on the parent material was retrieved from the Soil Database of China, available at http://globalchange.bnu.edu.cn (Pang et al. 2022). Field trips were conducted to validate the accuracy of the data sources.

Statistical analysis

Bioconcentration factor

The bioconcentration factor (BCF) is calculated as follows (Xu et al. 2024; Pan et al. 2022):

$$BCF = \frac{Se_{\text{grain}}}{Se_{\text{soil}}}$$

where Se_{grain} (mg·kg^{-1}) is Se concentration in rice grains, and Se_{soil} (mg·kg^{-1}) is Se concentration in paddy soil. This parameter illustrates the potential transfer of Se from paddy soil to the rice's edible portion.

Path analysis

Regression analysis and significance tests were utilized to determine the primary factors influencing the concentrations of Se in soil, grain, and BCF, thereby elucidating the interactive effects on these variables. Within the context of Partial Least Squares (PLS) path models, the overall influence on Se_{soil}, Se_{grain} concentration, and Se BCF was characterized by a combination of direct and cumulative indirect impacts. The calculation of indirect impacts involved multiplying the path coefficients that govern the direct effects among variables. The summation of these products yielded the cumulative total indirect effect, thereby providing a comprehensive perspective on the mechanism of influence (Xu et al. 2024; Pan et al. 2022; Xiao et al. 2020b).

Before analysis, we initially assessed all data for normality and homogeneity in SPSS 26.0. Pearson's correlation analysis was employed for co-occurrence networks and correlation heatmaps in SPSS 26.0 and RStudio 4.2.2.

The pairwise Pearson's correlation between soil chemical properties (SOM, CEC, and pH), essential micronutrient elements (Cu, Zn, and Mn) of paddy soils and rice grains, geographical and climate factors (elevation, slope, aspect, DFW, MAT, and MAP), and dependent variable (Se_{soil} concentration, Se_{grain} concentration, and Se BCF) were determined in SPSS 26.0. Then a combined correlation diagram was visualized with the ggcor package in RStudio 4.2.2 (Sunagawa et al. 2015). For the analysis of differences in Se_{soil} concentration, Se_{grain} concentration, and Se BCF among various parent materials, a one-way ANOVA with the least significant difference (LSD) test was employed in SPSS 26.0, with significance set at $p < 0.05$. To predict the most influential variables for Se_{soil} concentration, Se_{grain} concentration, and Se BCF, we employed the stepwise multiple linear regression method based on the influencing factors in SPSS 26.0 (Xu et al. 2024; Xiao et al. 2020b). PLS analysis was conducted in RStudio 4.2.2. The production of Figs. 1 and 2 was carried out in ArcGIS 10.8. Figures 3, 5, and 6 were created using Origin 2021. Figure 4 was produced in RStudio 4.2.2.

Results

Spatial distribution of Se in paddy soil and rice grains

The Se concentration observed in paddy soil exhibited a notable range, spanning from 0.005 to 29.2 mg·kg^{-1}. The calculated average concentration of Se within paddy soil was 0.55 mg·kg^{-1}, with a corresponding median value of 0.46 mg·kg^{-1}. Similarly, the Se concentration identified within rice grains spanned a range from 0.001 to 3.312 mg·kg^{-1}. The mean concentration of Se in rice grains was computed as 0.058 mg·kg^{-1}, while the median value stood at 0.046 mg·kg^{-1} (refer to Table 1). Conforming to the soil and rice grain Se classification standards outlined by Xu et al. (2020) and Dinh et al. (2018), the analysis identified 83,141 soil survey sites and 75,468 rice grain survey sites located within Se-rich regions, constituting 64.45% and 58.51% of the total, respectively (Table 2). Notably, there were 50,984 sites exhibiting Se concentration in both paddy soil and rice grains corresponding to the Se-rich classification, accounting for 39.52% of the total survey sites. A smaller subset, consisting of 114 sites, demonstrated excessive Se concentration within both paddy soil and rice grains, representing 0.09% of the total survey sites. Furthermore, 20,905 sites displayed Se concentration in paddy soil and rice grains that did not attain the Se enrichment threshold, equating to 16.21% of the overall sampling sites.

Utilizing the fundamental principles of ordinary Kriging, Fig. 2 provides a visual representation of the Se distribution across soil and rice grains. Notably, the Se concentration within paddy soil across Hunan Province is generally high. Specifically, the western, northeastern, and southern regions of the province are positioned within the intersection of the Se-sufficient and Se-rich distribution areas. Intriguingly, pockets of Se-excessive

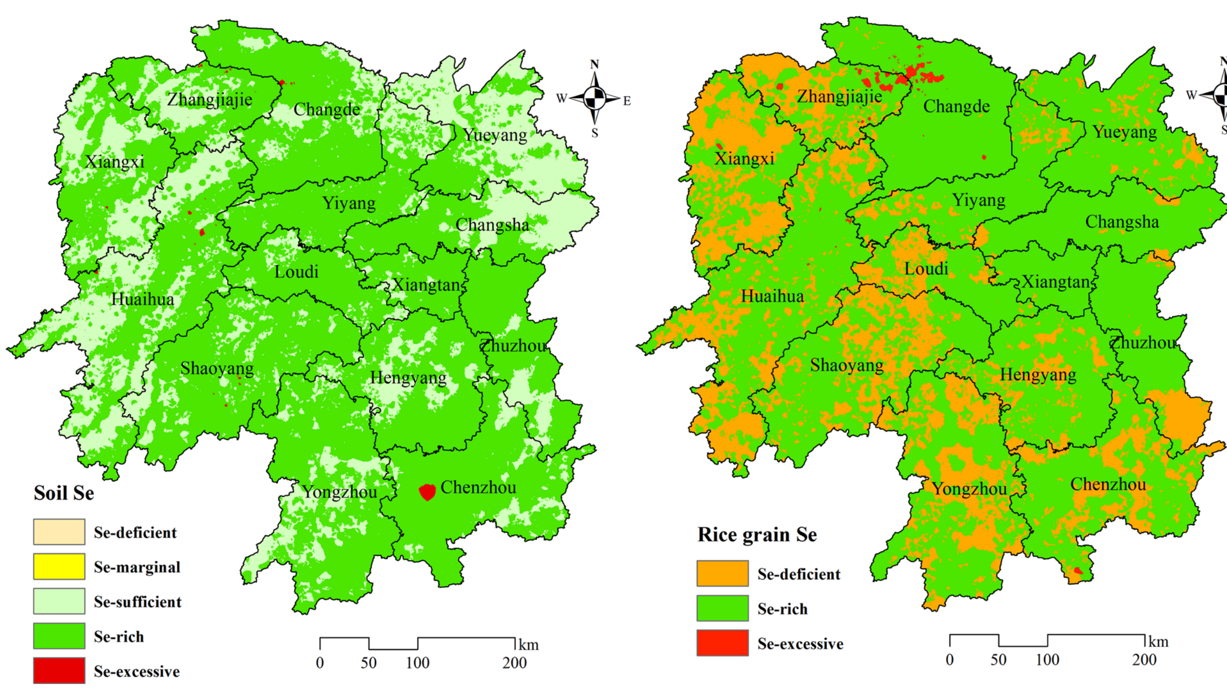

Fig. 2 Distribution of paddy soil Se and rice grain Se in Hunan Province

paddy soils are discernible in specific locales, notably along the borders of Zhangjiajie and Changde, the central and southern reaches of western Hunan, the northern expanses of Huaihua, the central and southern portions of Shaoyang, as well as the central and western territories of Chenzhou. Se-rich rice grains are widely distributed in Hunan Province. Key production areas encompass Changde, central Yiyang, Changsha, Xiangtan, the northern sector of Zhuzhou, and the southeastern district of Loudi. A minor scattering of Se-excessive rice grains is observable in locales such as Zhangjiajie, northern Changde, central Hunan, and southwestern Chenzhou. Notably, these regions align with Se-excessive paddy soil zones, albeit with slight discrepancies in positioning.

The soil chemical properties, essential micronutrient elements, geographical and climate factors

Figure 3 and Table 1 provide a comprehensive overview of the examined variables, encompassing soil chemical properties (SOM, CEC, and pH), essential micronutrient concentrations (Se, Cu, Zn, and Mn) within both paddy soil and rice grains, geographical and climatic factors (elevation, slope, aspect, DFW, MAT, and MAP), as well as Se BCF. The mean Se concentration in soil was notably elevated, registering at 0.55 mg·kg^{-1}. Conversely, the average concentration of Se detected in rice grains stood at 0.058 mg·kg^{-1}, while the average BCF of Se was calculated to be 0.12. Notably, Se_{soil}, Se_{grain}, and BCF exhibited coefficients of variation (CV) of 84.26%, 199.52%, and 156.45%, respectively. These values underscore significant spatial differentiation across the study area.

With respect to the soil properties, the average pH level measured 6.02, indicative of acidic paddy soil conditions. The mean SOM concentration was high at a value of 33.74 g·kg^{-1}. The CV associated with SOM demonstrated a relatively mild variation, at 38.8%. However, there were discernible spatial variations in the CV values for soil concentration of Zn (Zn_{soil}), Mn (Mn_{soil}), and Cu (Cu_{soil}), quantified at 114.97%, 125.83%, and 124.58%, respectively.

Concurrently, the study area showcased a mean MAT of 17.5 °C, coupled with a mean MAP of 1690 mm. Furthermore, the elevation of paddy soil emerged as relatively low, averaging at 252.9 m. The inclination of the

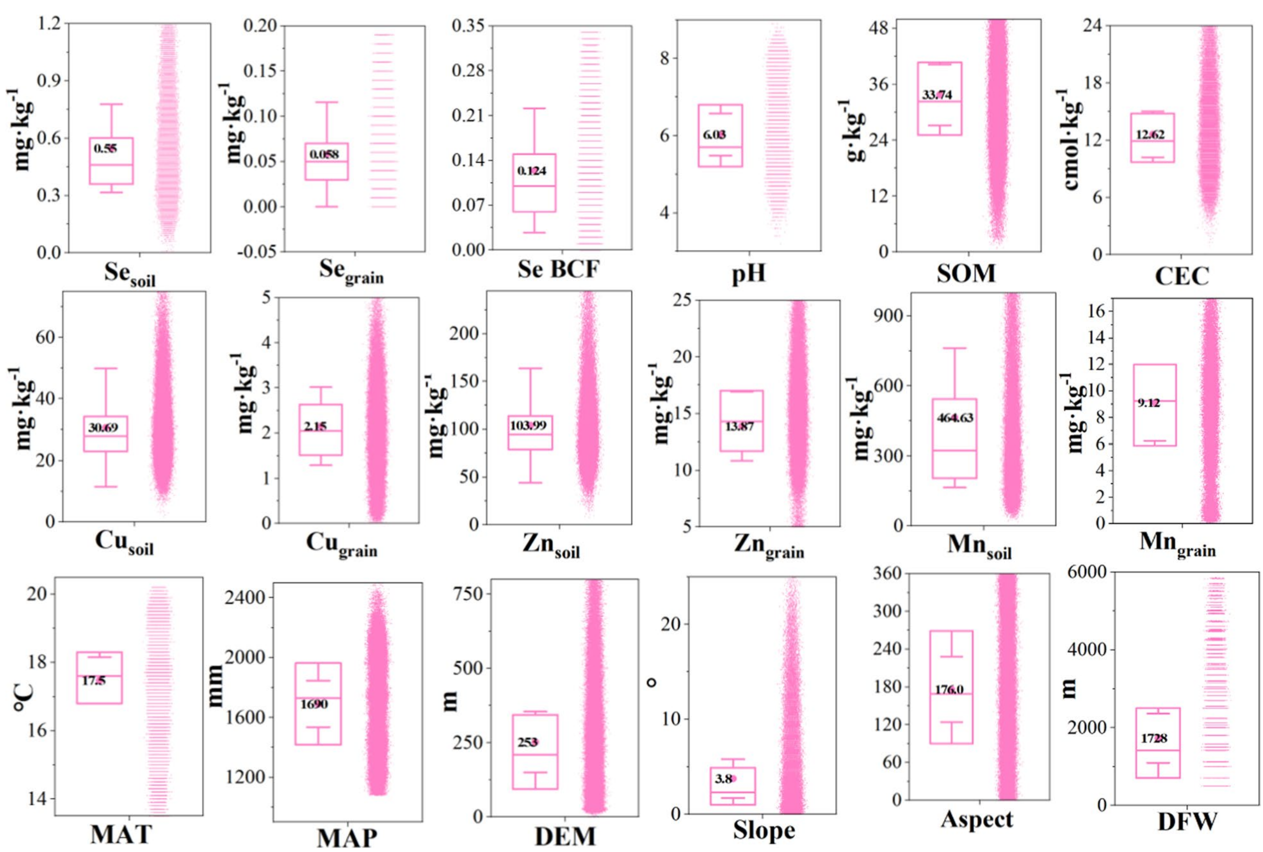

Fig. 3 Descriptive statistics of box plots and jittered strip plots for soil chemical properties (SOM, CEC, and pH), essential micronutrient elements in paddy soil and rice grains (Se, Cu, Zn, and Mn), geographical and climate factors (elevation, slope, aspect, DFW, MAT, and MAP), and BCF. The coupled rectangles and values labeled in the plots depict the average values

paddy soil terrain exhibited a relatively gradual slope, with an average angle of 3.8°. Geographically, the aspect of paddy soil exhibited a uniform and well-balanced distribution. Notably, the average distance from paddy soil to adjacent rivers or water bodies was determined to be approximately 1472 m.

Relationships between driving factors with Se_{soil}, Se_{grain}, and Se BCF

The intricate relationships involving Se_{soil}, Se_{grain}, Se BCF, and an array of digitized drivers encompassing soil essential micronutrient elements, as well as geographical and climate factors are shown in Fig. 4. Upon subjecting

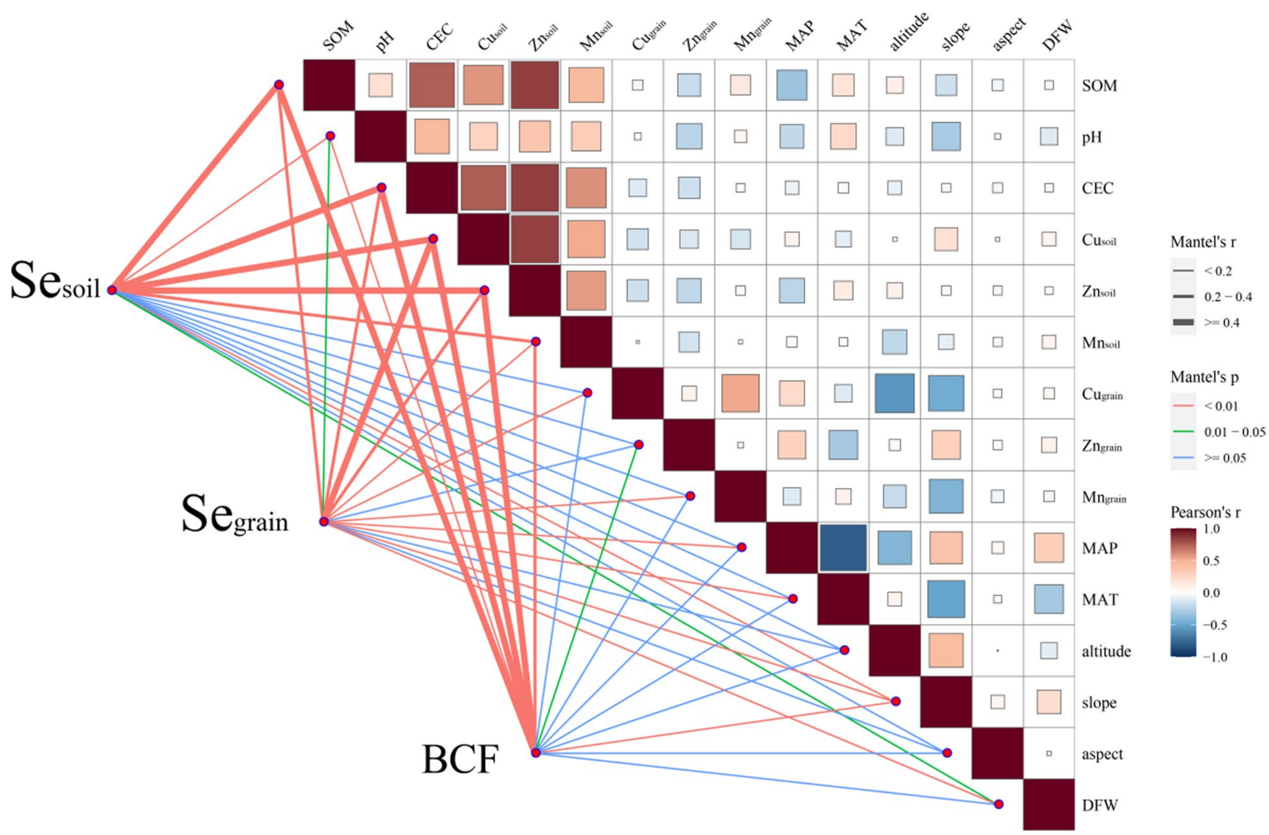

Fig. 4 Within this heatmap analysis, intricate correlations amongst an assortment of factors are graphically unveiled. The matrix delves into the interplay between soil chemical properties (SOM, CEC, and pH), essential micronutrient elements (Cu, Zn, and Mn), as well as geographical variables (elevation, slope, aspect, MAT, MAP, and distance from water), in relation to Se_{soil}, Se_{grain} concentration, and Se BCF. This visual representation effectively distills intricate patterns of relationships, elucidating the mutual influences between these factors and the examined variables

Table 2 Survey sites number of soil and rice grain on their Se classification standard

	Se classification standard ($mg \cdot kg^{-1}$)	Number of survey sites	Proportion of total survey sites (%)
Se concentration in soil	Se-deficient (< 0.125)	296	0.23
	Se-marginal (0.125–0.175)	1017	0.79
	Se-sufficient (0.175–0.40)	43,882	34.02
	Se-rich (0.40–3.00)	83,141	64.45
	Se-excessive (> 3.00)	656	0.51
Se concentration in rice grain	Se-deficient (< 0.04)	52,472	40.68
	Se-rich (0.04–0.30)	75,468	58.51
	Se-excessive (> 0.30)	1052	0.82

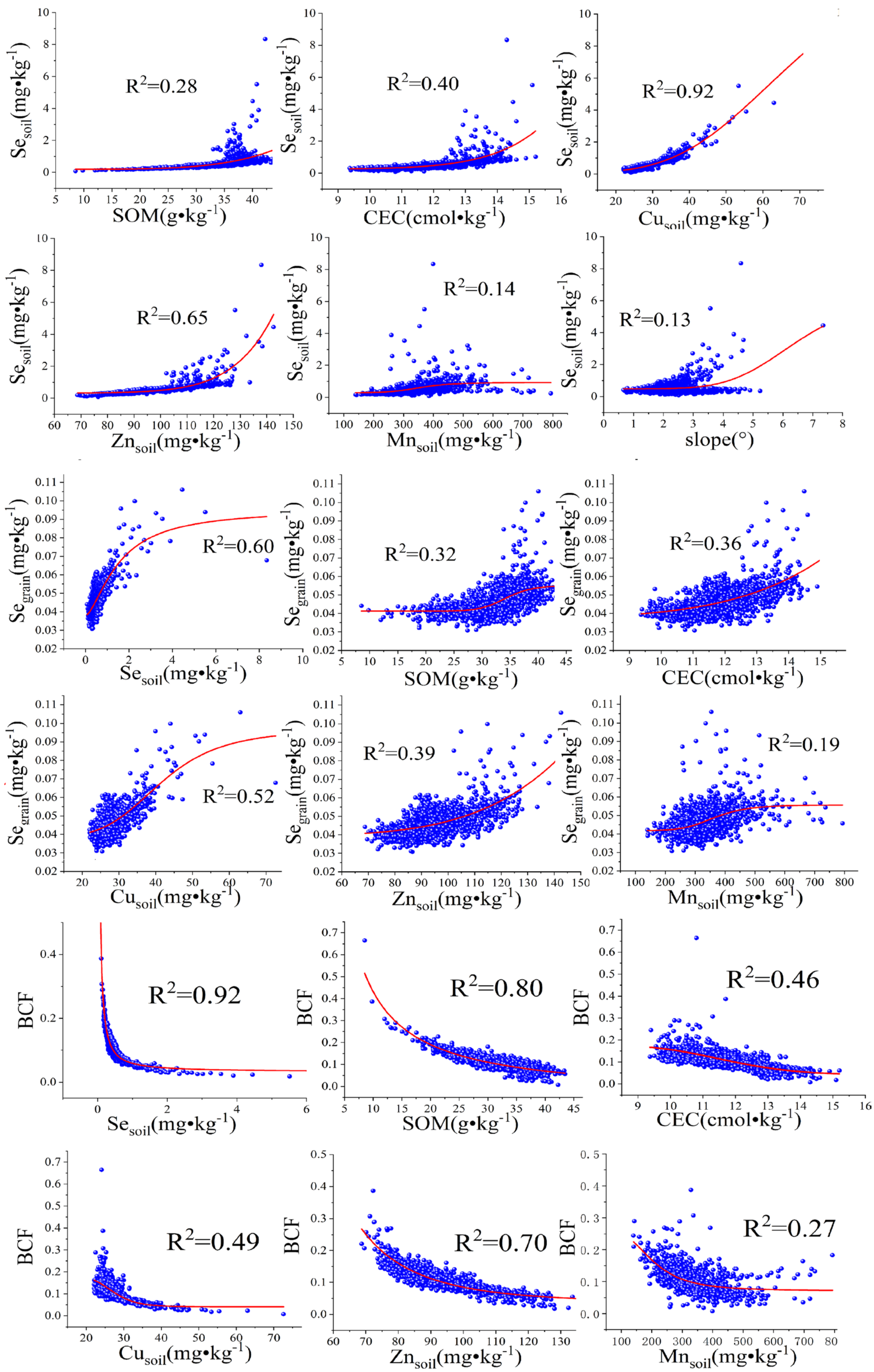

Fig. 5 Relationships between the soil chemical properties (SOM and CEC), essential micronutrient elements (Cu, Zn, and Mn), geographical factors (slope), and Se_{soil}, Se_{grain} concentration, and Se BCF

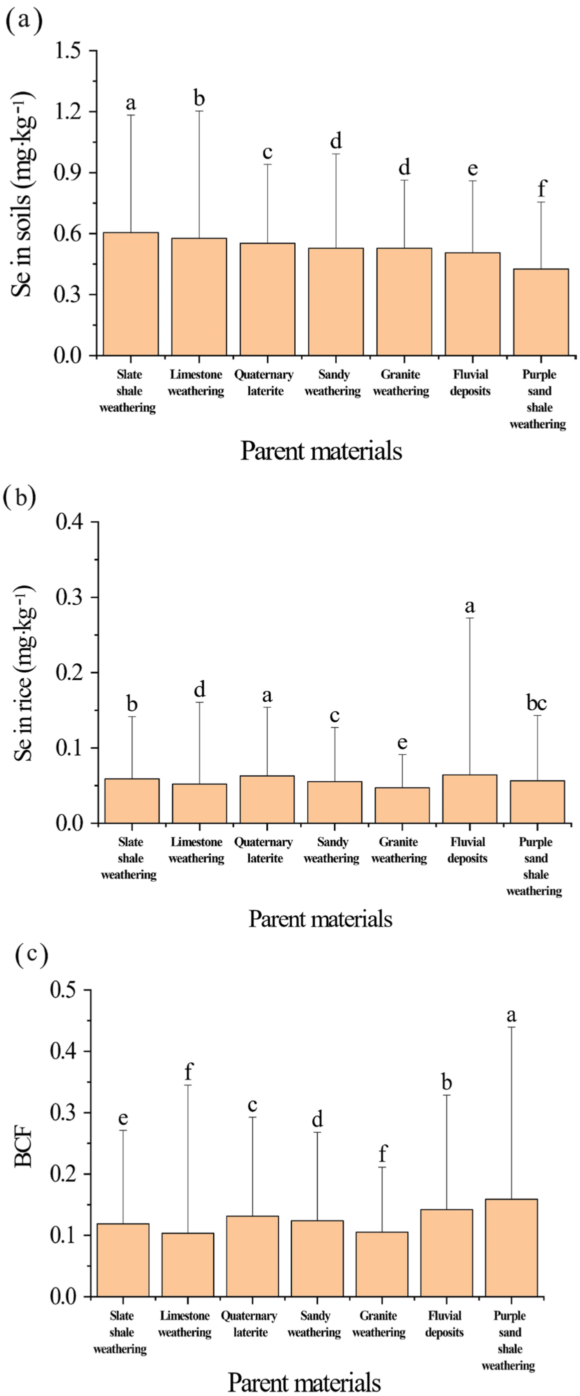

Fig. 6 The paddy soil Se concentration (**a**), rice grain Se concentration (**b**) and Se BCF (**c**) in different parent materials

the dataset to the Mantel test, compelling associations emerged. Notably, the Se_{soil} concentration showcased statistically significant correlations with a range of variables, including SOM, CEC, Cu_{soil}, Zn_{soil}, Mn_{soil}, pH, and slope ($p < 0.01$). Additionally, a correlation with DFW was observed ($p < 0.05$). Similarly, the Se_{grain} concentration demonstrated statistically significant associations with several drivers. These encompassed SOM, CEC, Cu_{soil}, Zn_{soil}, Mn_{soil}, Cu_{grain}, Mn_{grain}, MAP, MAT, slope, and DFW ($p < 0.01$), along with a correlation with pH ($p < 0.05$). Likewise, Se BCF exhibited pronounced connections ($p < 0.01$) with an ensemble of factors, including SOM, pH, CEC, MAP, Cu_{soil}, Zn_{soil}, Mn_{soil}, and slope. Notably, the influence of Zn_{grain} on Se BCF emerged as significant ($p < 0.05$), adding further nuance to the relationships.

In accordance with the significant findings highlighted in Fig. 4, a segmentation approach was employed for nonlinear fitting of the extensive dataset (Fig. 5). Notably, variables including SOM, CEC, Cu_{soil}, Zn_{soil}, Mn_{soil} concentration, MAP, and slope exhibited a positive correlation with the Se_{soil} concentration, with R^2 values spanning from 0.13 to 0.92. Moreover, the Se_{grain} concentration demonstrated a positive correlation with SOM, CEC, Se_{soil} concentration, Cu_{soil} concentration, Zn_{soil}, and Mn_{grain} concentration, with R^2 values spanning from 0.19 to 0.60. In a distinctive contrast, Se BCF exhibited negative correlations with SOM, CEC, Se_{soil}, Se_{grain}, Zn_{soil}, Cu_{soil}, and Mn_{soil} concentration, with R^2 values spanning from 0.16 to 0.92. These discernible outcomes distinctly illustrated that the influencing factors—Se_{soil}, Se_{grain} concentration, and Se BCF—manifested themselves in diverse ways.

Furthermore, it's worth highlighting that the intricate influence of soil parent materials was uniquely instrumental and hence not substituted by digitization. Consequently, the distinct effects of parent materials on Se_{soil}, Se_{grain}, and Se BCF were examined and individually discussed, unveiling a comprehensive understanding of their contributions. The analysis of average Se_{soil}, Se_{grain} concentration, and Se BCF across the seven distinct parent materials showcased varying ranges. For Se_{soil}, the average concentration ranged between 0.43 and 0.61 mg·kg^{-1}, whereas for Se_{grain}, it fell within the range of 0.047 to 0.064 mg·kg^{-1}. Furthermore, the average Se BCF exhibited a range from 0.10 to 0.16 (Fig. 6). However, their distribution followed different patterns. Notably, the average Se_{soil} concentration within slate shale weathering (0.61 mg·kg^{-1}) significantly exceeded that of purple sand shale weathering (0.43 mg·kg^{-1}). Similarly, the average Se_{grain} concentration within fluvial deposits (0.064 mg·kg^{-1}) markedly surpassed that of granite weathering (0.047 mg·kg^{-1}). Additionally, the average Se BCF of purple sand shale weathering (0.16) was significantly higher than that of limestone weathering (0.10) ($p < 0.05$). These findings collectively underscored the pronounced impact of different parent materials on Se_{soil}, Se_{grain}, and Se BCF.

Direct and indirect effects of driving factors on Se_{soil}, Se_{grain} concentration, and BCF

The PLS path models elucidated 74%, 53%, and 73% of the total variance in Se_{soil} concentration, Se_{grain} concentration, and Se BCF, respectively. The outcomes revealed the following: SOM exerted both direct and indirect effects on Se_{soil} concentration, whereas Cu_{soil} concentration displayed solely direct effects, and Zn_{soil} concentration along with CEC manifested only indirect effects (Fig. 7a). Similarly, CEC and Cu_{soil} concentration exhibited both direct and indirect influences on Se_{grain} concentration, whereas Se_{soil} exhibited only direct influences, and SOM and Zn_{soil} concentration showcased exclusively indirect effects (Fig. 7b). Meanwhile, SOM concentration and CEC showcased direct and indirect influences on Se BCF, whereas Cu_{soil} exhibited only direct influences, and Se_{soil} and Zn_{soil} concentration displayed solely indirect effects (Fig. 7c).

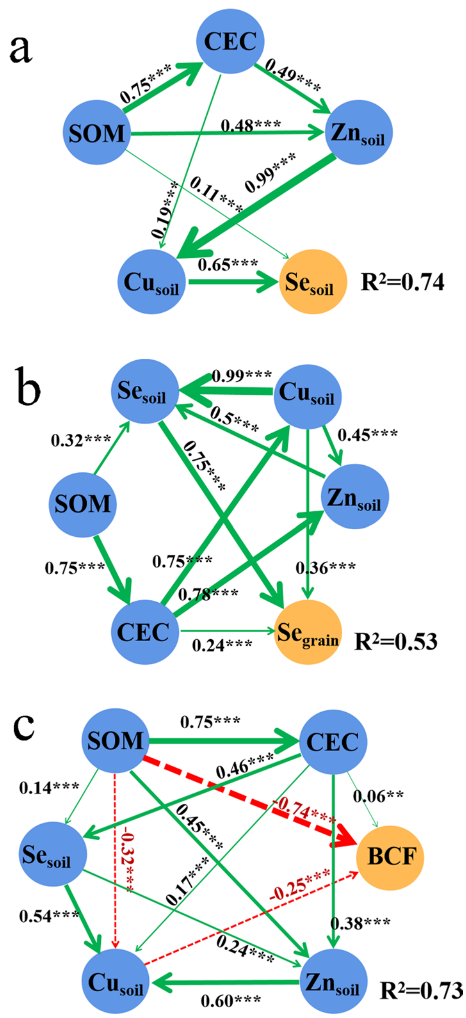

Fig. 7 PLS path models describing the relationships between soil chemical properties and essential micronutrient elements on Se_{soil} concentration (**A**), Se_{grain} concentration (**B**), and Se BCF (**C**). R^2 values represent the proportion of the variance explained for the internal variable. Green and continuous arrows show a positive correlation ($p < 0.01$). Red and dashed arrows show a negative correlation ($p < 0.01$). The numbers following the containing variables indicate the explained percentage of the variance by their predictors. The numbers on the arrows were the standardized path coefficients

Meanwhile, Table 3 illustrated the direct, indirect, and overall influences of these factors on Se_{soil}, Se_{grain}, and Se BCF. Among these, SOM, Zn_{soil} concentration, Cu_{soil} concentration, and CEC emerged as the most pivotal influencing factors on Se_{soil} concentration, reflecting notably high positive effects. Correspondingly, CEC, Cu_{soil} concentration, SOM, and Se_{soil} concentration emerged as the most crucial influencing factors on Se_{grain} concentration, with significant positive effects. Additionally, SOM, Cu_{soil}, Se_{soil}, Zn_{soil}, and CEC appeared as the most influential factors on Se BCF (Table 3).

Prediction of Se_{soil}, Se_{grain} concentration, and BCF by the dominant influencing factors

Multiple regression analysis was conducted with the dependent variables (Se_{soil}, Se_{grain} concentration, and Se BCF) and independent variables (soil properties), leading to the formulation of prediction models as depicted in Table 4. The R^2 values, serving as indicators of the explanatory strength of the predictive models, were determined. In our study, the R^2 values for Se_{soil}, Se_{grain}, and Se BCF were calculated as 0.81, 0.52, and 0.73, respectively ($p < 0.001$). Notably, Cu_{soil} and CEC emerged as primary influencing factors for soil Se, jointly accounting for 81% of the variance. Similarly, Cu_{soil} and Se_{soil} emerged as key contributors to rice grain Se, collectively accounting for 52% of the variance. Meanwhile, Se_{soil} and SOM took center stage as the primary determinants of Se BCF, collectively explaining 73% of the variance.

Discussion

Accumulation of Se in paddy soil and rice grains

The average Se concentration in paddy soil in Hunan Province (0.55 $mg \cdot kg^{-1}$) surpassed the background soil levels in both China (0.29 $mg \cdot kg^{-1}$) and the global context (0.40 $mg \cdot kg^{-1}$), indicating a considerable enrichment (Fordyce et al. 2007, 2013; Chen et al. 1991). In accordance with the Se classification criteria outlined by Dinh et al. (2018), the findings indicate a predominantly favorable Se level in the paddy soils of Hunan Province (Fig. 2a). Concurrently, the mean concentration of Se in rice grains was measured at 0.058 $mg \cdot kg^{-1}$, comfortably meeting the criteria for Se-rich rice grains (0.04–0.30 $mg \cdot kg^{-1}$) as stipulated by the National Standard Agency of China (GB/T 22499–2008; Farooq et al. 2019).

Table 3 Direct, indirect, and total effects of influencing factors on the Se_{soil} concentration, Se_{grain} concentration, and Se BCF

	Influencing factors	Direct effects	Total indirect effects	Total effects
Se_{soil} concentration	SOM	0.11***	0.68***	0.79***
	CEC		0.46***	0.46***
	Cu_{soil}	0.65***		0.65***
	Zn_{soil}		0.70***	0.70***
Se_{grain} concentration	SOM		0.50***	0.50***
	CEC	0.24***	0.32***	0.56***
	Se_{soil}	0.25***		0.25***
	Cu_{soil}	0.36***	0.19***	0.55***
	Zn_{soil}		− 0.12**	− 0.12**
Se BCF	SOM	− 0.74***	− 0.10***	− 0.84***
	CEC	0.06**	− 0.18**	− 0.12**
	Se_{soil}		− 0.17***	− 0.17***
	Cu_{soil}	− 0.25***		− 0.25***
	Zn_{soil}		− 0.15***	− 0.15***

Table 4 Multiple regression model to predict Se_{soil}, Se_{grain} concentration and Se BCF

	Independent variables	Multiple regression models	*p*	R^2
Se_{soil} concentration	CEC, Cu_{soil}	$Se_{soil} = 0.107 \times Cu_{soil} - 0.092 \times CEC - 1.398$	< 0.001	0.81
Se_{grain} concentration	Cu_{soil}, Se_{soil}	$Se_{grain} = 0.001 \times Cu_{soil} + 0.005 \times Se_{soil} + 0.02$	< 0.001	0.52
Se BCF	Se_{soil}, SOM	$BCF = - 0.005 \times SOM - 0.018 \times Se_{soil} + 0.292$	< 0.001	0.73

Notably, a significant portion of the area exhibited Se-rich in rice grains (Fig. 2b).

The analytical outcomes spotlighted a robust positive correlation between Se concentration in rice grains and that in soil. Interestingly, the BCF of Se exhibited a pronounced negative correlation with soil Se, indicating that the concentration of Se in rice grains is likely to rise with elevated soil Se levels. However, as soil Se concentrations increase, the overall Se BCF tends to decrease.

Factors affecting Se accumulation in paddy soil

Parent materials constitute the foundational material and primary source of surface soil Se, traditionally considered the pivotal origin of Se in soil. In a general context, sedimentary rocks usually contain higher Se levels than igneous rocks (Pang et al. 2022; Liu et al. 2021b; Sharma et al. 2015), elucidating the highest concentration of Se in slate shale weathering within this study. Owing to the limited adsorption capacity of clay particles, Se in soils derived from fluvial deposits might be vulnerable to losses through rainwater percolation and groundwater leaching, ultimately resulting in significantly lower Se concentration compared to other soil types. Purple sand shale weathering soils, primarily comprised of purple soil, are characterized by loose structure, susceptibility to erosion, and shallow soil depth, all factors contributing to poor Se accumulation (Chen et al. 2021). This suggests that soils originating from fluvial deposits and purple sand shale weathering exhibit low Se concentration. Nevertheless, as pedogenic processes advance, the significance of soil chemical and physical properties in determining soil Se concentration becomes increasingly pronounced, gradually diminishing the influence of parent materials (Xu et al. 2024; Xiao et al. 2020b; Gabos et al. 2014). Paddy soil, being matured soil subjected to long-term flooding, is significantly influenced by external factors, which in turn greatly affect Se accumulation.

SOM assumes a crucial role in Se mobility and bioavailability. Research underscores SOM as a pivotal factor impacting soil Se concentration (Xu et al. 2024; Liu et al. 2021a). In our study, a notable positive correlation emerged between SOM and Se_{soil} (Fig. 5). Its mechanism was that, in the soil, Se is transformed into a form that can be directly absorbed and utilized by plants; after plant enrichment and decay, it combines with humus in a difficult migrating form, so that Se is fixed in the soil, and the increase of SOM concentration can also improve soil structure, which is easier to make Se adsorption (Xu et al. 2024; Wang et al. 2022). Thus, higher SOM concentration is synonymous with elevated Se concentration in soil.

Furthermore, the expansive dispersion and absorption surface of humus empowers SOM to influence Se enrichment in paddy soils through the sequential path of SOM → CEC → Zn_{soil} → Cu_{soil} → Se (Fig. 7a). Concurrently, a robust positive correlation was identified between CEC and Se_{soil} concentration (Fig. 5). The Mantel test validated significant relationships between Se_{soil} concentration and the values of Cu_{soil}, Zn_{soil}, and Mn_{soil} (Fig. 4). Existing studies suggest that selenite (SeO_3^{2-}) prevails under conditions of high soil moisture and intense aeration (Chang et al. 2019). Consequently, in paddy soils, cations (Zn^{2+} and Cu^{2+}) may form complexes with the primary Se forms (SeO_3^{2-}) to foster Se adsorption. Additionally, this relationship could be attributed to the homology or coexistence of Zn, Cu, and Se, which could stem from the same parent rock (Xu et al. 2024; Song et al. 2020; Prasad 2008). Within the context of paddy soils, Zn_{soil} and Cu_{soil} may influence Se_{soil} concentration indirectly through the cascade SOM → CEC → Zn_{soil} → Cu_{soil} → Se (Fig. 7a).

Furthermore, the study revealed that soil Se concemtration had a minor correlation with pH, suggesting that alterations in pH alone may not substantially impact soil Se concentration (Fig. 5). Additionally, climate and topography, which can impact Se accumulation in soil (Pang et al. 2022), showed minimal correlation with Se_{soil} in our study (Fig. 5). This could be attributed to the limited variability in MAT (CV = 7.81) and MAP (CV = 18.31) within the study area (Table 1). Furthermore, the regression analysis indicated that elevation, slope, aspect, and DFW did not exert a definitive influence on Se_{soil}.

Significantly, the prediction model illuminated CEC and Cu_{soil} concentration as primary contributors to elevated Se accumulation in paddy soils, accounting for an impressive 81% of the contribution (Table 4). Hence, even though natural and anthropogenic factors impact paddy soil Se, CEC and Cu_{soil} concentration can to some extent regulate Se accumulation in Se-enrichment practices. These findings not only offer theoretical guidance but also practical techniques for devising effective control measures to address Se challenges in paddy soils.

Factors affecting Se accumulation in rice grains

Our findings suggest that the influence of the seven different parent materials on Se concentration in rice grains is relatively minor (Fig. 6). However, these parent matterials do not emerge as significant factors affecting Se_{grain} (Fig. 7). PLS path model analysis revealed that SOM, CEC, Se_{soil}, Cu_{soil}, and Zn_{soil} hold key positions in determining the Se concentration in rice grains (Fig. 7). It's essential to highlight that Se_{soil} functions as the primary source of Se_{grain}. In our study, a highly significant positive correlation between Se_{grain} and Se_{soil} was observed (Fig. 5), indicating that, under equivalent conditions, higher soil Se concentration corresponds to increased Se absorption by rice. Previous research has demonstrated the influence of Zn_{soil} and Cu_{soil} on Se_{grain} (Xu et al. 2020). Referring to Sect. "Factors affecting Se accumulation in paddy soil", we can deduce that SOM and CEC play a role on Zn_{soil}, Cu_{soil}, and Se_{soil} concentration. As a result, these factors could indirectly influence Se_{grain} concentration through the pathway of SOM/CEC → Zn_{soil}/Cu_{soil}/Se_{soil} → Se in rice grains (Fig. 7b).

Furthermore, our study revealed that rice grain Se concentration displayed a weak correlation with pH, suggesting that alterations in pH alone do not exert a direct influence on Se_{grain} concentration (Fig. 5). Additionally, the correlation between Se_{grain} concentration and geographical and climatic factors in this study was modest. Significantly, Cu_{soil} and Se_{soil} concentrations were identified as primary contributors to elevated Se accumulation in rice grains, accounting for 52% of the contribution according to the prediction model (Table 4). Consequently, despite the interplay of natural and anthropogenic factors on rice grain Se concentration, Cu_{soil} and Se_{soil} concentration possess the capacity to regulate rice grain Se accumulation to a certain extent, particularly in Se enhancement practices. These findings offer both theoretical and practical insights for formulating efficient strategies to address Se challenges in rice grains.

Factors affecting Se bioavailability in paddy soils

With the exception of granite weathering and limestone weathering, the performance of Se BCF exhibited significant variability across different parent materials ($p < 0.05$). This aligns with other research findings; for example, Xiao et al. (2020a) observed that the determining factor for Se bioavailability in dryland soils, cultivated with corn, was heavily reliant on the parent material (specifically limestone and clasolite). However, it is deduced from the analysis of the PLS path model that the significance of soil parent materials in influencing BCF diminishes. This could be attributed to the long history of paddy soil cultivation (Nayak et al. 2007). The susceptibility of Se bioavailability in paddy soils to the influence of parent materials is relatively low. Existing studies have affirmed that soil physicochemical properties play a role in shaping the distribution of Se bioavailability (Liu et al. 2021a). In this study, curve fitting analysis (Figs. 4 and 7) has indicated a negative correlation between Se BCF and various factors. This observation aligns with the results reported by Ullah et al. (2019) and Fernández-Martínez and Charlet (2009). Se can form Se-cation-organic matter complexes by complexing with SOM and metal (Dinh et al. 2018) via the metal bridge (Martin et al. 2017;

Sharma et al. 2010). As plants are unable to directly absorb water-insoluble forms of Se such as metallic selenide and elemental Se, Se bioavailability in paddy soil with high levels of Zn, Cu, and SOM might be lower compared to soils with lower concentrations of these elements (Xu et al. 2024; Natasha et al. 2018).

Furthermore, neither climatic conditions (MAP and MAT) nor geographical factors (elevation, slope, aspect, and DFW) demonstrated substantial associations with BCF in this study.

Management of Se in paddy soil-rice system

The bioconcentration factor (BCF) serves as a useful tool for assessing the potential transfer of elements from soil to plants and is also instrumental in gauging the pollution status of toxic elements (Xu et al. 2024; Pan et al. 2022; Natasha et al. 2018). In our study, the BCF ranged from 0.00007 to 19.6, with a mean value of 0.12. These values were notably lower in comparison to the results of Jiao et al. (2022) whose research reported a Se BCF of 0.89. The underlying reason lies in the relatively low concentration of effective Se in paddy soil, which consequently restricts plants' capacity to absorb a substantial amount of this effective Se (Xu et al. 2024; Pang et al. 2022; Haug et al. 2007).

Interestingly, despite the limited effective Se_{soil}, the rice grains in this study area exhibited a notably rich Se concentration (0.058 $mg \cdot kg^{-1}$). This value surpasses the average Se concentration (0.02 $mg \cdot kg^{-1}$) of rice observed across China (Fang et al. 2008). Consequently, in the pursuit of either sustaining or further augmenting the Se-rich status of rice in Hunan Province, two avenues present themselves. Firstly, the application of foliar Se fertilizer could be employed to augment the available source of Se absorption for rice plants (Gui et al. 2022; Liu et al. 2021a). Secondly, enhancing the utilization efficiency of Se in rice soil can be achieved through the regulation and management of variables such as SOM, CEC, Zn_{soil}, and Cu_{soil}. It should be noted that 0.51% of soil sampling points and 0.82% of rice sampling points in Hunan Province are in a state of selenium excess. In these areas, it is possible to consider planting root crops or legumes with low Se BCF, such as potatoes, sugar beets, soybeans, and peas (Xu et al. 2024; Wu et al. 2012).

Conclusions

The distribution, accumulation, and bioavailability of Se in the paddy soil-rice system were investigated in this study, along with an evaluation of its influencing factors in the Hunan rice-producing area. The average Se concentration in paddy soil in Hunan Province was found to be 1.9 times higher than the background soil level in China. It was observed that 64.45% of soil samples and 58.51% of rice samples reached Se-rich levels (0.40–3.00 $mg \cdot kg^{-1}$ and 0.04–0.30 $mg \cdot kg^{-1}$, respectively). The study revealed significant Se accumulation in rice grains. Attention should be given to preventing Se poisoning in areas with excessive Se levels (< 0.1%). Moreover, Se concentrations in both soil and rice grains were notably higher in the western, central, and southern regions of Hunan Province compared to the eastern and northern regions. Factors such as SOM, CEC, Cu_{soil}, and Zn_{soil} were identified to have a significant positive influence on Se levels in both soil and rice grains. Among these factors, SOM and Cu_{soil} were highlighted as the primary determinants of Se concentration in soil, consequently impacting Se levels in rice grains as well. These findings underscore the importance of considering these factors when aiming to enhance Se concentration in rice or other cereal crops.

Acknowledgements
Not applicable.

Author contributions
Guiduo Shang: Data curation, Investigation, Software, Formal analysis, Writing—original draft; Writing—review & editing. Weijun Zhou: Conceptualization, Project administration, Funding acquisition, Supervision, Writing—review & editing. Rui Liu: Data curation, Software. Yuzhou Zhou: Formal analysis, Investigation. Zhangqian Xu: Methodology, Formal analysis, Software. Haojie Cui: Formal analysis, Methodology. Yixiang Cai: Formal analysis, Methodology.

Funding
We gratefully acknowledge the support provided by the National Modern Agricultural Technology System Construction Project (CARS-26).

Availability of data and materials
The datasets used and/or analyzed during the current study are available from the corresponding author on reasonable request.

Declarations

Ethics approval and consent to participate
Not applicable.

Consent for publication
Not applicable.

Competing interests
The authors declare that they have no competing interests.

Received: 13 December 2023 Accepted: 24 May 2024
Published online: 28 June 2024

References

Ahmad M, Lee SS, Lee SE, Al-Wabel MI, Tsang DC, Ok YS (2017) Biochar-induced changes in soil properties affected immobilization/mobilization of metals/metalloids in contaminated soils. J Soils Sediments 17:717–730
Beladel B, Nedjimi B, Mansouri A, Tahtat D, Belamri M, Tchanchane A, Benamar MEA (2013) Selenium content in wheat and estimation of the selenium daily intake in different regions of Algeria. Appl Radiat Isot 71(1):7–10
Chang C, Yin R, Wang X, Shao S, Chen C, Zhang H (2019) Selenium translocation in the soil-rice system in the Enshi seleniferous area, Central China. Sci Total Environ 669:83–90

Chen J, Wei F, Zheng C, Wu Y, Adriano DC (1991) Background concentrations of elements in soils of China. Water Air Soil Pollut 57:699–712
Davies BE, Houghton NJ (1983) The selenium content of welsh soils with special reference to bedrock and contamination from sulphide ores. Minerals Environ 5(2):67–70
Dinh QT, Li Z, Tran TAT, Wang D, Liang D (2017) Role of organic acids on the bioavailability of selenium in soil: a review. Chemosphere 184:618–635
Dinh QT, Cui Z, Huang J, Tran TAT, Wang D, Yang W, Liang D (2018) Selenium distribution in the Chinese environment and its relationship with human health: a review. Environ Int 112:294–309
Elrashidi MA (2018) Selenium distribution for soils derived from Mancos shale in Gunnison and Uncompahgre River Basins, West-Central Colorado. Commun Soil Sci Plant Anal 49:1083–1091
Fang Y, Wang L, Xin Z, Zhao L, An X, Hu Q (2008) Effect of foliar application of zinc, selenium, and iron fertilizers on nutrients concentration and yield of rice grain in China. J Agric Food Chem 56(6):2079–2084
Farooq MU, Tang Z, Zheng T, Asghar MA, Zhu J (2019) Cross-talk between cadmium and selenium at elevated cadmium stress determines the fate of selenium uptake in rice. Biomolecules 9(6):247
Favorito JE, Eick MJ, Grossl PR, Davis TZ (2017) Selenium geochemistry in reclaimed phosphate mine soils and its relationship with plant bioavailability. Plant Soil 418(1–2):1–15
Fernández-Martínez A, Charlet L (2009) Selenium environmental cycling and bioavailability: a structural chemist point of view. Rev Environ Sci Biotechnol 8:81–110
Fordyce F (2007) Selenium geochemistry and health. Ambio 36(1):94–97
Fordyce FM (2013) Selenium deficiency and toxicity in the environment. In: Selinus O (ed) Essentials of medical geology. Springer, Dordrecht. pp 375–416
Gabos MB, Alleoni LRF, Abreu C (2014) Background levels of selenium in some selected Brazilian tropical soils. J Geochem Explor 145:35–39
Gui J-Y, Rao S, Huang X, Liu X, Cheng S, Xu F (2022) Interaction between selenium and essential micronutrient elements in plants: a systematic review. Sci Total Environ 853:158673
Hao L, Zhang J, Zhang S, Ma S, Li B, Long J, Luo K (2021) Distribution characteristics and main influencing factors of selenium in surface soil of natural selenium-rich area: a case study in Langao County, China. Environ Geochem Health 43:333–346
Haug A, Graham RD, Christophersen OA, Lyons GH (2007) How to use the world's scarce selenium resources efficiently to increase the selenium concentration in food. Microb Ecol Health Dis 19(4):209–228
Hawrylak-Nowak B, Matraszek R, Pogorzelec M (2015) The dual effects of two inorganic selenium forms on the growth, selected physiological parameters and macronutrients accumulation in cucumber plants. Acta Physiol Plant 37:1–13
Jiao L, Zhang L, Zhang Y, Wang R, Lu B, Liu X (2022) Transcriptome analysis provides new insight into the distribution and transport of selenium and its associated metals in selenium-rich rice. Environ Pollut 301:118980
Kieliszek M, Bano I, Zare H (2022) A comprehensive review on selenium and its effects on human health and distribution in Middle Eastern countries. Biol Trace Element Res 200:971–987
Kushwaha A, Goswami L, Lee J, Sonne C, Brown RJ, Kim KH (2022) Selenium in soil-microbe-plant systems: sources, distribution, toxicity, tolerance, and detoxification. Crit Rev Environ Sci Technol 52(13):2383–2420
Li Z, Liang D, Peng Q, Cui Z, Huang J, Lin Z (2017) Interaction between selenium and soil organic matter and its impact on soil selenium bioavailability: a review. Geoderma 295:69–79
Liu Y, Chen J, Pan L, Wu T, Yang B, Xing Y, Liao Q, Liang P, Jiang Z (2018) Studies on causes and influential factors of selenium-rich soil in Xunyu plain. Soils 50(6):1139–1144
Liu N, Wang M, Zhou F, Zhai H, Qi M, Liu Y, Li Y, Zhang N, Ma Y, Huang J, Ren R, Liang D (2021a) Selenium bioavailability in soil-wheat system and its dominant influential factors: a field study in Shaanxi province, China. Sci Total Environ 770:144664
Liu YL, Tian XL, Liu R, Liu SL, Zuza AV (2021b) Key driving factors of selenium-enriched soil in the low-Se geological belt: a case study in Red Beds of Sichuan Basin, China. Catena 196:104926
Natasha, Shahid M, Niazi NK, Khalid S, Murtaza B, Bibi I, Rashid MI (2018) A critical review of selenium biogeochemical behavior in soil-plant system with an inference to human health. Environ Int 234:915–934
Nayak DR, Babu YJ, Adhya TK (2007) Long-term application of compost influences microbial biomass and enzyme activities in a tropical Aeric Endoaquept planted to rice under flooded condition. Soil Biol Biochem 39(8):1897–1906
Ning Y, Hu M, Chen S, Zhang F, Yang X, Zhang Q, Gong Y, Huang R, Liu Y, Chen F, Pei L, Guo X, Kang L, Wang X, Zhang Y, Wang X (2022) Investigation of selenium nutritional status and dietary pattern among children in Kashin-Beck disease endemic areas in Shaanxi Province, China using duplicate portion sampling method. Environ Int 164:107255
Pan SF, Ji XH, Xie YH, Liu SH, Tian FX, Liu XL (2022) Influence of soil properties on cadmium accumulation in vegetables: thresholds, prediction and pathway models based on big data. Environ Pollut 304:119225
Pang YJ, He J, Niu X, Song TJ, Fu L, Liu K, Bi ER (2022) Selenium distribution in cultivated Argosols and Gleyosols of dry and paddy lands: a case study in Sanjiang Plain, Northeast China. Sci Total Environ 836:155528
Prasad MN (2008) Trace elements as contaminants and nutrients: consequences in ecosystems and human health. John Wiley & Sons
Qvarforth A, Lundgren M, Rodushkin I, Engstrom E, Paulukat C, Hough RL, Moreno-Jimenez E, Beesley L, Trakal L, Augustsson A (2022) Future food contaminants: an assessment of the plant uptake of technology-critical elements versus traditional metal contaminants. Environ Int 169:107504
Rayman MP (2002) The argument for increasing selenium intake. Proc Nutr Soc 61(2):203–215
Sharma P, Ofner J, Kappler A (2010) Formation of binary and ternary colloids and dissolved complexes of organic matter, Fe and As. Environ Sci Technol 44(12):4479–4485
Song TJ, Cui G, Su XS, He J, Tong SZ, Liu Y (2020) The origin of soil selenium in a typical agricultural area in Hamatong River Basin, Sanjiang Plain, China. Catena 185:104335
Song Y, Wang C, Linderholm HW, Fu Y, Cai W, Xu J, Chen D (2022) The negative impact of increasing temperatures on rice yields in southern China. Sci Total Environ 820:153262
Sunagawa S, Coelho LP, Chaffron S, Kultima JR, Labadie K, Salazar G, Velayoudon D (2015) Structure and function of the global ocean microbiome. Science 348(6237):1261359
Tan JA, Zhu WY, Wang WY, Li RB, Hou SF, Wang DC, Yang LS (2002) Selenium in soil and endemic diseases in China. Sci Total Environ 284:227–235
Ullah H, Liu G, Yousaf B, Ali MU, Irshad S, Abbas Q, Ahmad R (2019) A comprehensive review on environmental transformation of selenium: recent advances and research perspectives. Environ Geochem Health 41:1003–1035
Wang C, Zhang Z, Zhang J, Tao F, Chen Y, Ding H (2019) The effect of terrain factors on rice production: a case study in Hunan Province. J Geog Sci 29:287–305
Wang Z, Huang W, Pang F (2022) Selenium in soil–plant–microbe: a review. Bull Environ Contam Toxicol 108:167–181
Wu D, Fang KM, Shen HF, Wan T, Lu J (2012) Comparative study on selenium-enriching ability of different types of vegetables in Leping City of Jiangxi. Acta Agriculturae Jiangxi 24(7):23–24
Xiao KC, Lu LF, Tang JJ, Chen H, Li DJ, Liu YX (2020a) Parent material modulates land use effects on soil selenium bioavailability in a selenium-enriched region of southwest China. Sci Total Environ 744:140925
Xiao KC, Tang JJ, Chen H, Li DJ, Liu YX (2020b) Impact of land use/land cover change on the topsoil selenium concentration and its potential bioavailability in a karst area of southwest China. Sci Total Environ 707:136041
Xu Y, Li Y, Li H, Wang L, Liao X, Wang J, Kong C (2018) Effects of topography and soil properties on soil selenium distribution and bioavailability (phosphate extraction): a case study in Yongjia county, China. Sci Total Environ 633:240–248
Xu YF, Hao Z, Li YH, Li HR, Wang L, Zang ZF, Liao XY, Zhang R (2020) Distribution of selenium and zinc in soil-crop system and their relationship with environmental factors. Sci Total Environ 699:134250
Xu ZQ, Zhou WJ, Zhou YZ, Cui H, Liu R, Shang GD (2024) Factors controlling accumulation and bioavailability of selenium in paddy soils: a case study in Luxi County, China. Environ Pollut 348:123196
Yang G, Wang S, Zhou R, Sun S (1983) Endemic selenium intoxication of humans in China. Am J Clin Nutr 37:872–881
Yang H, Yang X, Ning Z, Kwon SY, Li M-L, Tack FM, Kwon EE, Rinklebe J, Yin R (2022) The beneficial and hazardous effects of selenium on the health of the soil-plant-human system: an overview. Sci Total Environ 822:126876

Zou M, Zhou S, Zhou Y, Jia Z, Guo T, Wang J (2021) Cadmium pollution of soil-rice ecosystems in rice cultivation dominated regions in China: a review. Sci Total Environ 798:149339

Publisher's Note